

Sage-modified polydimethylsiloxane applied as antibacterial wound dressing material

Sara Sarraj^{1), *} (ORCID ID: 0000-0002-1691-884X), Małgorzata Szymiczek¹⁾ (0000-0001-5574-6545),
Dariusz Jędrejek²⁾ (0000-0001-5585-9697), Agata Soluch²⁾ (0000-0001-6355-1414), Roksana Kurpanik³⁾ (0000-0002-7943-7509)

DOI: <https://doi.org/10.14314/polimery.2024.1.4>

Abstract: Materials based on polydimethylsiloxane have been developed with antibacterial activity and mechanical properties required for wound treatment. Sage herb (raw, modified, and polyphenol extract) was used as a filler in an amount of 5 and 10% by weight. Physicochemical, mechanical, and biological properties were examined. The results indicate a beneficial effect of sage modification on the tested properties.

Keywords: polydimethylsiloxane, antimicrobial activity, wound dressing, salvia, polyphenols.

Polidimetylosiloksan modyfikowany szalwią jako antybakteryjny materiał opatrunkowy

Streszczenie: Na bazie polidimetylosiloksanu opracowano materiały o działaniu przeciwbakteryjnym i właściwościach mechanicznych wymaganych przy leczeniu ran. Jako napełniacz zastosowano ziele szalwii (surowe, modyfikowane i ekstrakt polifenolowy) w ilości 5 i 10% mas. Zbadano właściwości fizykochemiczne, mechaniczne i biologiczne. Wykazano korzystny wpływ modyfikacji szalwii na badane właściwości.

Słowa kluczowe: polidimetylosiloksan, działanie przeciwbakteryjne, opatrunki na rany, szalwia, polifenole.

Wounds are defined as a disruption of the epidermis continuity due to physical or thermal trauma. Depending on the duration of the healing process, two types of wounds can be distinguished: acute and chronic [1]. Both types of wounds can pose a threat to the organism if not appropriately treated. One main reason for prolonged wound healing is skin and soft tissue infections (SSTIs) [2]. Bacterial invasions can be caused by the lack of hygiene and suitable environmental conditions, e.g., moisture. This creates ideal conditions that promote bacterial growth, leading to the formation of a resistant biofilm and subsequent severe health problems. Therefore, the wound dressings industry is constantly researching different approaches to acquire bandage materials exhibiting antibacterial or bacteriostatic properties.

Thus far, more than 3000 types of wound dressings are available, divided into two groups: traditional and modern. Traditional wound dressings include gauze dressings of woven and non-woven polyester or cotton, which provide a certain degree of bacterial protection [3]. Modern wound dressings are constantly developing to promote wound healing and act as a barrier against the penetration of infectious pathogens. Bioactive agents (drugs and inorganic nanoparticles) incorporated into the dressing's material limit the proliferation of bacteria. These dressings come in various forms depending on the production material. Moreover, unlike traditional dressings, modern ones can employ dermal elements with fibroblasts on a collagen matrix that stimulates wound growth [1].

One of the materials used for wound dressing production is polydimethylsiloxane (PDMS). Its high gas permeability makes it advantageous in the industry due to the separation of gases from the material [4, 5]. Moreover, PDMS retains its flexibility over a wide temperature range. This is essential from the sterilization process point of view. In addition, PDMS is hydrophilic, which impedes bacterial adhesion. Although the material is biocompatible, its inertness also extends to microbes. Therefore, researchers are consistently developing new PDMS-based materials that exhibit antimicrobial properties.

Nanoparticles are widely used as a modifier of PDMS to obtain antimicrobial material. In one approach, scien-

¹⁾ Silesian University of Technology, Faculty of Mechanical Engineering, Department of Theoretical and Applied Mechanics, Konarskiego 18A, 44-100 Gliwice, Poland.

²⁾ Institute of Soil Science and Plant Cultivation—State Research Institute, Department of Biochemistry and Crop Quality, Czartoryskich 8, 24-100 Puławy, Poland.

³⁾ AGH University of Kraków, Faculty of Materials Science and Ceramics, Department of Biomaterials and Composites, Mickiewicza 30, 30-059 Kraków, Poland.

^{*} Author for correspondence: sara.sarraj@polsl.pl

tists incorporated silver nanoparticles into 3D-printed polydimethylsiloxane to promote infected wound healing and exhibit antibacterial activity [6]. Similar studies were conducted by Li *et al.*, who introduced silver nanowires and caffeic acid to a silicone matrix [7]. Another work studied the impact of incorporating ZnO into PDMS [8]. Tests proved higher resistance of ZnO/PDMS to *Escherichia coli* compared to ZnO by itself. Other works proved the favorable influence of similar fillers [9-12]. In a different approach, researchers developed polyhexamethylenebiguanide (a polymer used for disinfecting wounds) loaded PDMS, which exhibited antibacterial activity against multiple Gram-positive and Gram-negative bacteria [13]. However, as science proceeds, scientists are researching new methods of antibacterial material development. In works found in the literature, researchers coated or incorporated herbal extracts into silicone [14-17]. These studies proved the beneficial impact of herbal extracts on the biocidal properties of the obtained materials. Nevertheless, limited works study the effect of the direct incorporation of herbs into the PDMS matrix. Authors' previous research studied the impact of incorporating thyme and sage into silicone [18]. This work continues the previous study, focusing mainly on sage composites.

This research aims to develop bio-based polydimethylsiloxane composites exhibiting antibacterial activity while maintaining the required operational properties. This approach employed incorporating sage prepared using different methods into the PDMS matrix and studying the impact on selected properties. As a proof-of-concept, an antimicrobial activity assessment was conducted.

EXPERIMENTAL PART

Materials

Medical-grade platinum-crosslinked polydimethylsiloxane (PDMS) was used as the matrix (Dragon Skin 30, Smooth-on, Inc., Macungie, PA, USA). Dried sage herb (*Salvia officinalis*) was used as a modifier. Three different preparations were employed. The first was raw sage, where the herb was additionally dried at $20\pm 1^\circ\text{C}$ for 24 h

and ground using a two-blade grinder (Fig. 1a). For the second preparation, the previously obtained herb was sieved using Mutliserw sieve shaker (Multiserw-Morek, Brzeźnica, Poland) to collect particles smaller than $150\ \mu\text{m}$. The sieved filler was wetted with 90% ethanol for 4 h and dried at $30\pm 1^\circ\text{C}$ for 24 h (Fig. 1b). The third filler was sage polyphenolic extract (Fig. 1c). For this purpose, finely ground raw sage herb (ca. 150 g) was twice extracted with boiling MiliQ water (3.5 L + 1.5 L) for 5 min. After combining, the extracts were filtered on a Schott funnel and centrifuged (4500 rpm, 5°C ; Sigma 3-26 KL, Osterode am Harz, Germany) for 10 min. The extraction efficiency was 35.8%. The aqueous extract was found to contain large amounts of polar impurities (such as carbohydrates and organic acids), as indicated by liquid chromatography-mass spectrometry (LC-MS) analysis. The phenolic compounds were further purified by solid-phase extraction on a short column ($12 \times 5\ \text{cm}$) filled with Cosmosil C18-Prep bed ($140\ \mu\text{m}$; Nacalai Tesque Inc., Kyoto, Japan). Methanol and formic acid (to a final concentration of 2% and 0.1% (v/v), respectively) were added to the extract, and it was filtered again and loaded (separately in 5 portions) onto a column stabilized with 2% MeOH (v/v) and washed with 2% MeOH (v/v) containing formic acid. Compounds of interest were eluted with 60% MeOH (v/v). The resulting polyphenol fractions were combined and then lyophilized (Gamma 2-16 LSC, Christ, Osterode am Harz, Germany) after evaporation of the solvent on a vacuum evaporator (Laborota 20, Heidolph, Schwabach, Germany) at 40°C . The procedure yielded 9.19 g of sage polyphenolic extract.

Making of composites

The composites and the reference material were prepared following the producer's instruction (silicone base to catalyst = 1:1). The fillers were incorporated into the PDMS matrix in ratio of 5 and 10 wt% (Fig. 2). However, it should be noted that for sage extract composites, the amount of incorporated filler was equal to the quantity of polyphenolic compounds in unmodified sage. The calculation was based on the efficiency of the extraction



Fig. 1. Tested fillers: a) raw sage, b) modified sage, c) sage extract

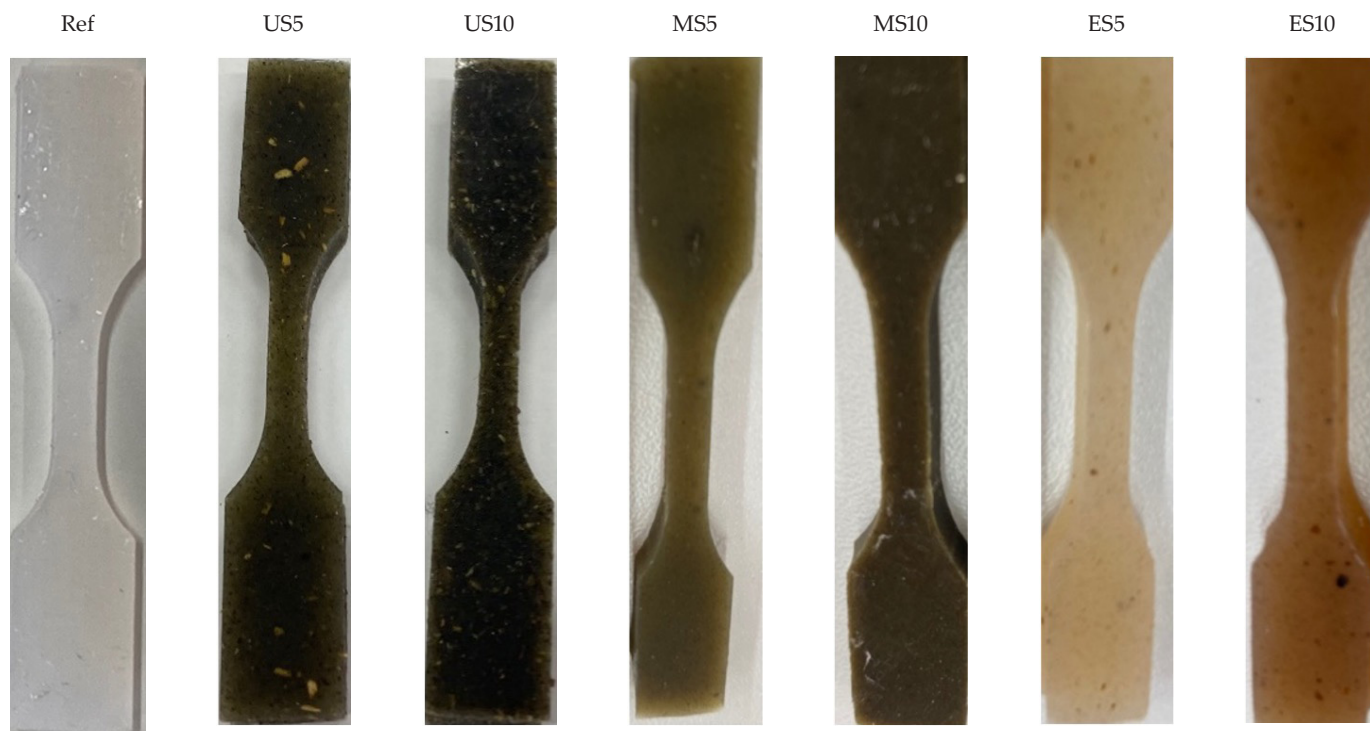


Fig. 2. Specimens for tensile tests

Table 1. Composition of the tested samples

Filler	Content, wt%	Symbol
Reference material	–	Ref
Raw sage	5	US5
	10	US10
Modified sage	5	MS5
	10	MS10
Polyphenolic extract	5	ES5
	10	ES10

process. This incorporation method was chosen to compare the impact of polyphenolic compounds apart from other compositions found in the tested herb. The compositions were mixed using a rotary mixer at 150 rpm and degassed for 4 min to remove trapped air bubbles, ensuring a homogeneous mixture. The materials were gravity-casted and allowed to cure at room temperature for 24 hours. Next, the materials were additionally cured at temp. $60 \pm 1^\circ\text{C}$ for 2 hours and conditioned at temp. $80 \pm 1^\circ\text{C}$ for another 2 hours. Table 1 shows the composition of the tested samples. All tests were carried out a temperature of 23°C and humidity around 50%.

Methods

Morphology

The topography of the filler grains was visualized using Zeiss Supra 35 microscope (Carl Zeiss AG, Oberkochen, Germany), where the samples were sputtered with gold

powder for 90 s before testing. The grain size and distribution were analyzed using Fritsch Analysette 22 Micro-Tec Plus (FRITSCH GmbH, Idar-Oberstein, Germany).

Phytochemical profiles

Phytochemical profiles of sage fillers were obtained using Thermo Ultimate 3000RS (Thermo Fischer Scientific, Waltham, MS, USA) ultra high-performance liquid chromatography (UHPLC) system equipped with a corona-charged aerosol detector (CAD), and coupled with Bruker Impact II HD (Bruker, Billerica, MA, USA) quadrupole-time of flight (Q-TOF) mass spectrometer (MS). Raw and modified herbs were previously extracted twice with 80 wt% methanol in an ultrasonic bath (Sonic-33, Polsonic, Poland) for 15 min (the final concentration of the extracts was 20 mg/mL). The lyophilized polyphenolic extract was dissolved in 80 wt% methanol at a 5 mg/mL concentration. After centrifugation (12,000 rpm, 3 min; MiniSpin, Eppendorf, Hamburg, Germany), the samples were separated on HSS C18 column (2.1×100 mm, $1.7 \mu\text{m}$, Waters, Milford, MA, USA) maintained at 45°C . A linear concentration gradient (from 5 to 85% for 30 min, at flow rate 0.4 mL/min) of the acetonitrile-water mixture (both acidified with 0.1% vol. formic acid) was used. MS analysis was performed in ESI(–) ion mode, using the following settings: scanning range – 50–1800 m/z; capillary voltage – 3.0 kV; dry gas flow – 10 L/min; dry gas temperature – 220°C ; nebulizer pressure – 2.0 bar; collision RF – 750 Vpp; transfer time – 100 μs ; prepulse storage time – 10 μs . The MS/MS spectra were registered using a collision energy of 35 eV with steps 60% and 120% of

CE. The acquired data were calibrated internally with sodium formate (10 mM solution in 50% vol. 2-propanol), which was injected into the ion source before the sample analysis. Data were processed using DataAnalysis 4.4 software (Bruker). Identification of chromatographic peaks was performed based on LC-PDA-MS/MS results and comparison with the internal metabolite database and the literature.

Density

The density of the materials was determined according to the ISO 1183-1 standard by the immersion method on an analytical balance equipped with a hydrostatic density measurement kit (Ohaus Adventurer Pro, Greifensee, Switzerland). All materials were tested 5 times on square samples with dimensions of $5 \times 5 \times 4$ mm.

Hardness

Shore A hardness was measured using Zorn Stendal durometer (Zorn Stendal, Saxony-Anhalt, Germany) according to the ISO 7619-1 standard. The hardness for each material was measured 5 times with minimal distance between measurements 10 mm. Tests were performed on the upper side of the casted materials to eliminate the influence of filler sedimentation.

Rebound resilience

The rebound resistance was determined using the Schob method (Heckert, Chemnitz, Germany) in accordance with the ISO 4662 standard. The measurements were repeated 5 times and the distance between the measurements was 15 mm. Samples with dimensions of $40 \times 50 \times 4$ mm were used. Before testing, the samples were conditioned.

Tensile properties

Static tensile properties were performed on a Shimadzu kN10D testing machine (Shimadzu Corporation, Kyoto, Japan) operating with Trapezium software in accordance with the ISO 527-2 standard. Based on a literature review [19, 20], the crosshead speed was determined to be

500 mm/min. A contact extensometer was used to record strain data. Dumbbell-shaped samples (Fig. 2) were prepared in accordance with the ISO 527-1 – type 5-B standard. The strength at break and elongation at break were determined based on the stress-strain curves.

Antibacterial activity

Antibacterial activity tests were performed on samples cut into discs with a diameter of 5 mm. The Kirby-Bauer diffusion test was performed in accordance with the protocol of the American Society of Microbiology, which used two commercial strains – Gram-positive *Staphylococcus aureus* (ATCC 29213) and Gram-negative *Escherichia coli* (ATCC 25922). These are mainly strains occurring in chronic wound infections [21–23]. Each strain was suspended in saline and the bacterial inoculum concentration was adjusted to a 0.5 McFarland turbidity ($\sim 1.5 \times 10^8$ CFU/mL) using a DEN-1B Benchtop densitometer (Grant Instruments, Cambridge, UK). The bacterial suspension was then spread on the agar surface using a sterile cotton swab. The evaluation was performed on Petri dishes filled with Mueller-Hinton agar to ensure stable growth of the tested strains. The samples were stored at $36 \pm 1^\circ\text{C}$ for 24 hours, after which the inhibition zone was measured.

RESULTS AND DISCUSSION

Morphology

The tested fillers are characterized by well-developed surface (Fig. 3). For both fillers, stomas and long net-like trichomes are visible. However, for modified sage grains, they are shorter due to the sieving process (Fig. 3b). Apart from trichomes, other irregularly shaped structures are observed. Although polydimethylsiloxane is hydrophobic, the surface of the grains provides mechanical adhesion to the matrix. It should be noted that at the microscopic level, no changes in the topography of sage grains (e.g. surface detachments) were observed after wetting with ethanol. The polyphenolic extract is characterized by grains of different shapes and sizes. Moreover, they have softer, homogeneous surfaces in contrast to the herb particles.

Laser diffraction of fillers (Fig. 4) shows the bimodal nature of unmodified sage (fine and large particles). For



Fig. 3. Images of sage fillers at a magnification of 2500 \times : a) before modification, b) after modification, c) polyphenolic extract

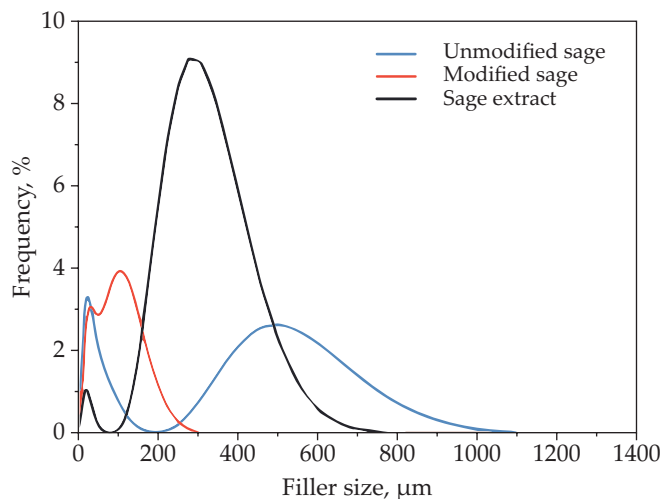


Fig. 4. Fillers particle size distribution

the modified sage the 90th percentile equals 131.21 µm, whereas for raw sage, it reaches 471.12 µm (about 4 times larger particles compared to the modified ones). For sage extract, the 90th percentile equals 380.71 µm; however, there was no apparent particle size dispersion. Moreover, it is worth noting that the extract is very soluble, and during testing, the grains dissolved with time. The size and topography of the grains have a significant impact on the properties of the tested materials.

UHPLC-MS analysis

The phytochemical profiles of sage materials are presented in Fig. 5. In general, the phytochemical profiles of the raw (Fig. 5a) and the modified (Fig. 5b) herb were not significantly different, i.e., they were dominated by diter-

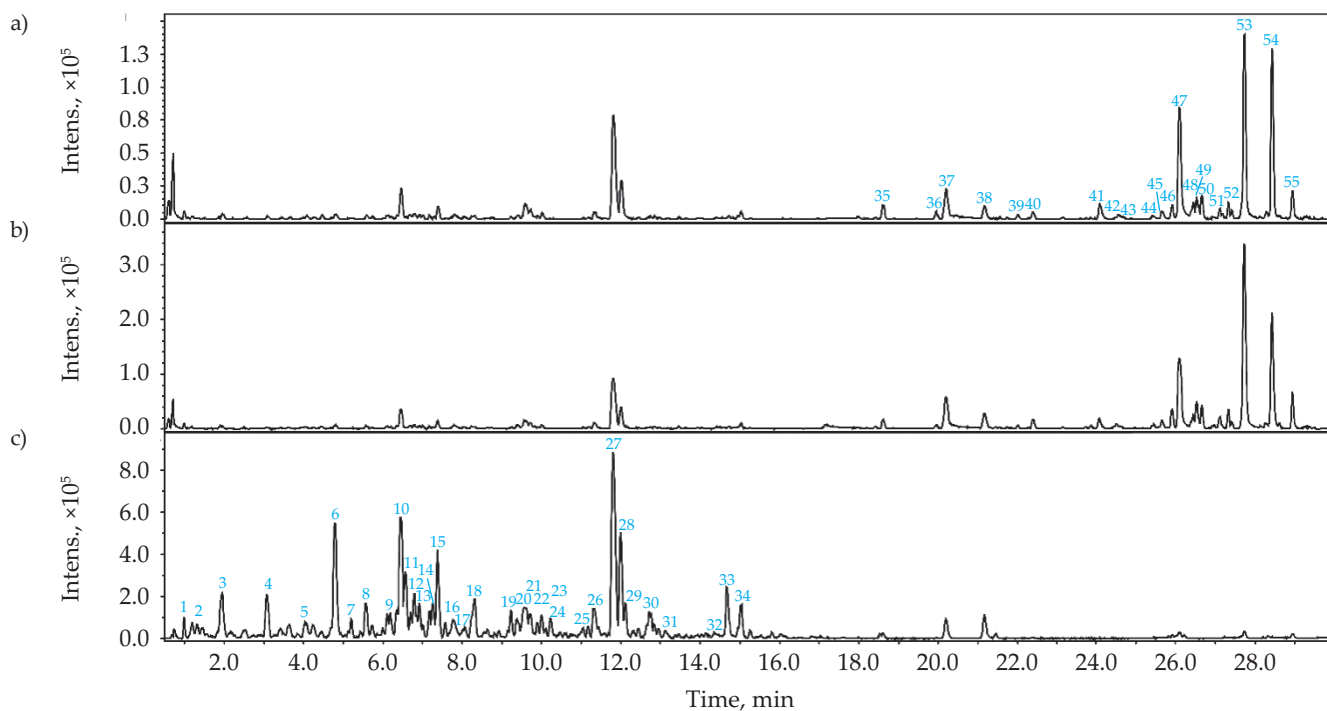


Fig. 5. UHPLC-QTOF-MS analysis of sage fillers: a) raw herb, b) modified herb, c) polyphenolic extract. Peak numbers correspond to table 2

penes (carnosol, carnosic acid, and methylated carnosic acid) and phenolic compounds (rosmarinic, salvianolic K and caffeic acids). In contrast, the extract enriched in polyphenols (Fig. 5c) consisted exclusively of this group of compounds, and the presence of terpenes, such as rosmanol, was traced. Most compounds identified in the samples were already confirmed to be present in the genus *Salvia*.

Density

The addition of fillers slightly increased the density of PDMS (Fig. 6) – the higher the filler content, the higher the density. However, these changes are within the error limits. The highest values are observed for modified sage composites. This is caused by the more even distribution of the filler (Fig. 2) compared to unmodified sage composites. The one-way ANOVA test performed shows a statistical difference between the composites $F(6,28) = 18.04$, $p < 0.05$; however, post-hoc analysis revealed that for MS5 and MS10 the changes were significant.

Hardness

Incorporating the tested fillers decreased the hardness of the matrix (Fig. 7); however, no obvious dependency between the filler type and content on the hardness results was found. The highest decrease is observed for raw sage composites, which is mainly related to the bimodal nature of the filler (smaller and larger particles). Moreover, smaller results scatter is observed compared to the other composites. This could be caused by the sedimentation of the filler's bigger particles. On the other hand, while testing mod-

Table 2. UHPLC-QTOF-MS/MS data of compounds detected in sage extracts

Peak No	RT min	[M-H] ⁻ m/z	MS/MS fragments	Formula [M-H] ⁻	Identity	Ref.
1	1.13	191.02	111.01	C ₆ H ₇ O ₇	citric acid	[24]
1	1.13	290.09	200.06; 128.04; 243.06	C ₁₁ H ₁₆ NO ₈	unidentified nitrogenous compound	
2	1.23	375.13	162.03; 177.06; 195.07	C ₁₇ H ₁₉ N ₄ O ₆	unidentified nitrogenous compound	
3	1.95	197.05	179.04; 135.04; 123.05	C ₉ H ₉ O ₅	3,4-dihydroxyphenyl lactic acid "danshensu"	[24-26]
4	3.11	181.05	163.04; 135.04; 119.05	C ₉ H ₉ O ₄	hydroxyphenyl-lactic acid	[25]
4	3.11	203.08	116.05; 186.06	C ₁₁ H ₁₁ N ₂ O ₂	tryptophan	
5	4.04	475.14	135.04; 293.09; 233.07	C ₂₀ H ₂₇ O ₁₃	benzoic acid glycoside	
6	4.80	179.03	135.04	C ₉ H ₇ O ₄	caffeic acid	[25, 27]
6	4.80	325.09	119.05; 163.04;	C ₁₅ H ₁₇ O ₈	<i>p</i> -coumaroyl quinic acid	[24]
7	5.18	405.21	225.15; 167.11	C ₁₉ H ₃₃ O ₉	unidentified	
8	5.72	223.06	181.05; 163.04	C ₁₁ H ₁₁ O ₅	sinapic acid	
8	5.72	535.11	181.05; 163.04; 223.06	C ₂₄ H ₂₃ O ₁₄	unidentified	
9	6.10	401.14	237.06; 269.10	C ₁₈ H ₂₅ O ₁₀	unidentified	
10	6.42	377.09	197.05; 161.02; 359.08	C ₁₈ H ₁₇ O ₉	salvianic acid C	[24, 28]
10	6.42	387.17	207.10	C ₁₈ H ₂₇ O ₉	tuberonic acid hexoside	[24]
11	6.86	431.19	385.19; 153.09; 205.12	C ₂₀ H ₃₁ O ₁₀	unidentified	
11	6.86	593.15	353.07; 473.11; 383.08	C ₂₇ H ₂₉ O ₁₅	isovitexin C-hexoside	
12	6.89	313.06	197.04; 153.06	C ₁₃ H ₁₃ O ₉	salicylate hexuronoside	
13	7.02	433.21	251.07; 207.14; 225.15; 163.11	C ₂₀ H ₃₃ O ₁₀	unidentified	
14	7.23	637.10	285.04; 351.06	C ₂₇ H ₂₅ O ₁₈	luteolin <i>O</i> -hexA-hexA	
15	7.41	225.11	147.08; 181.12	C ₁₂ H ₁₇ O ₄	tuberonic acid	[24]
16	7.71	477.07	301.03	C ₂₁ H ₁₇ O ₁₃	quercetin <i>O</i> -hexuronoside	[24]
16	7.71	537.16	281.07; 161.02; 519.15; 251.06	C ₂₅ H ₃₀ O ₁₃	phenolic glycoside	
17	8.05	463.09	301.03	C ₂₁ H ₁₉ O ₁₂	quercetin <i>O</i> -hexoside	[24]
17	8.05	623.13	285.04; 447.09	C ₂₇ H ₂₇ O ₁₇	luteolin <i>O</i> -hex-hexA	
18	8.33	375.17	329.16; 179.03; 161.05	C ₁₇ H ₂₇ O ₉	unidentified	
19	9.40	461.07	285.04	C ₂₁ H ₁₇ O ₁₂	luteolin <i>O</i> -hexuronoside	[24, 27]
20	9.65	461.07	285.04	C ₂₁ H ₁₇ O ₁₂	luteolin <i>O</i> -hexuronoside	[24, 27]
21	9.75	447.09	285.04	C ₂₁ H ₁₉ O ₁₁	luteolin <i>O</i> -hexoside	[24, 27, 29]
22	9.90	581.19	235.06; 563.18; 295.08; 193.05	C ₂₇ H ₃₃ O ₁₄	phenolic glycoside	
23	10.04	313.07	179.03; 135.04; 269.08	C ₁₇ H ₁₃ O ₆	salvianolic acid F	[24, 25, 28]
23	10.04	551.18	235.06;; 295.08; 193.05; 175.04	C ₂₆ H ₃₁ O ₁₃	phenolic glycoside	
24	10.24	389.09	193.05; 179.03; 161.02	C ₁₉ H ₁₇ O ₉	squamatic acid	
25	11.17	719.16	161.02; 197.05; 359.08	C ₃₆ H ₃₁ O ₁₆	sagerinic acid	[27, 29]
26	11.37	415.20	225.11	C ₂₀ H ₃₁ O ₉	hydroxyjasmonate glycoside	
26	11.37	445.08	269.05	C ₂₁ H ₁₇ O ₁₁	apigenin <i>O</i> hexsuronoside	[27]
27	11.78	359.08	197.05; 161.02; 179.04	C ₁₈ H ₁₅ O ₈	rosmarinic acid	[25, 27]
28	12.08	555.11	161.02; 359.08; 197.04; 295.06	C ₂₇ H ₂₃ O ₁₃	salvianolic acid K	[29, 30]
29	12.15	415.20	179.06; 281.07	C ₂₀ H ₃₁ O ₉	phenolic glycoside	
30	12.71	371.13	163.08; 285.04;; 179.06	C ₁₇ H ₂₃ O ₉	syringin	
31	13.50	269.04	-	C ₁₅ H ₉ O ₅	apigenin	[24, 29]

Table 2. cont.

Peak No	RT min	[M-H] ⁻ m/z	MS/MS fragments	Formula [M-H] ⁻	Identity	Ref.
32	14.37	373.09	197.05; 175.04; 179.04; 135.04	C ₁₉ H ₁₇ O ₈	methyl rosmarinate	[25, 29, 30]
33	14.70	569.13	339.05; 161.02; 193.05	C ₂₈ H ₂₅ O ₁₃	phenolic glycoside	
34	15.03	435.09	315.07; 297.06	C ₂₀ H ₁₉ O ₁₁	phenolic glycoside	
34	15.03	563.21	387.17; 175.04	C ₂₈ H ₃₅ O ₁₂	phenolic glycoside	
35	18.59	327.22	241.16; 229.14; 211.13	C ₁₈ H ₃₁ O ₅	trihydroxyoctadecadienoic acid	[24]
36	19.95	329.23	229.14; 211.13	C ₁₈ H ₃₃ O ₅	trihydroxyoctadecenoic acid	[24]
37	20.24	345.17	301.18; 283.17	C ₂₀ H ₂₅ O ₅	rosmanol isomer 1	[27, 29]
38	21.16	345.17	283.17	C ₂₀ H ₂₅ O ₅	rosmanol isomer 2	[27, 29]
39	22.00	307.19	235.13; 185.12; 211.13	C ₁₈ H ₂₇ O ₄	fatty acid derivative	
40	22.39	345.17	283.17	C ₂₀ H ₂₅ O ₅	rosmanol isomer 3	[27, 29]
41	24.12	311.22	223.17; 293.21	C ₁₈ H ₃₁ O ₄	octadecendioic acid	[24]
42	24.53	487.34	469.33; 425.34	C ₃₀ H ₄₇ O ₅	salvin A or B	[31]
43	24.64	331.19	285.19; 313.18	C ₂₀ H ₂₇ O ₄	carnosic acid isomer 1	[27, 29]
44	25.46	359.19	283.17	C ₂₁ H ₂₇ O ₅	rosmanol methyl ether isomer 1	
45	25.68	299.16	243.10	C ₁₉ H ₂₃ O ₃	unidentified	
45	25.68	687.32	299.17; 343.16	C ₄₀ H ₄₇ O ₁₀	unidentified	
46	25.91	359.19	283.17	C ₂₁ H ₂₇ O ₅	rosmanol methyl ether isomer 2	[29]
47	26.14	329.18	285.19	C ₂₀ H ₂₅ O ₄	carnosol	[27, 29]
48	26.45	293.21	275.20; 183.14	C ₁₈ H ₂₉ O ₃	oxooctadecadienoic acid isomer 1	
49	26.52	293.21	275.20; 183.14	C ₁₈ H ₂₉ O ₃	oxooctadecadienoic acid isomer 2	
50	26.69	343.15	315.16	C ₂₀ H ₂₃ O ₅	rosmadial	[27, 29]
51	27.13	315.20	285.19	C ₂₀ H ₂₇ O ₃	rosmaridiphenol	[26]
52	27.33	301.18	258.13	C ₁₉ H ₂₅ O ₃	unidentified	
53	27.74	331.19	287.20	C ₂₀ H ₂₇ O ₄	carnosic acid isomer 2	[27, 29]
54	28.48	345.21	286.19; 301.22	C ₂₁ H ₂₉ O ₄	carnosic acid methyl ether	[27, 29]
55	28.93	317.21	287.20	C ₂₀ H ₂₉ O ₃	fatty acid derivative	

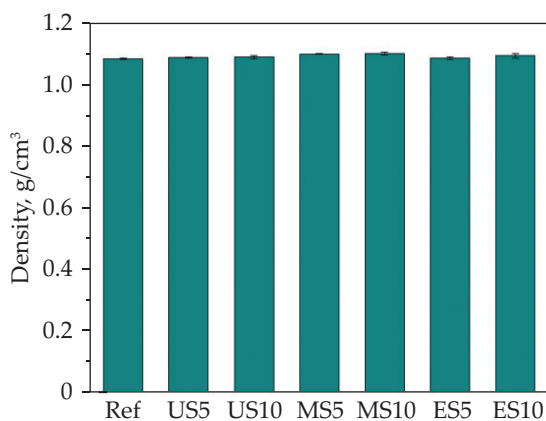


Fig. 6. The effect of the fillers on PDMS density

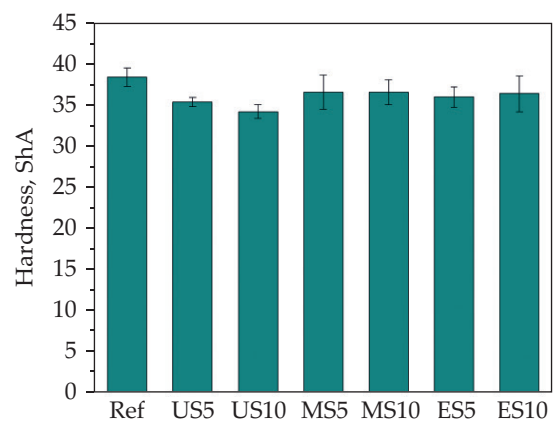


Fig. 7. The effect of the fillers on PDMS hardness

ified sage-filled and extract-filled materials, light-weight agglomerates seen on Fig. 2 were encountered resulting in varied values. In modified sage composites, the hardness decreased by only 4.6% due to the uniform distribution of the grains in the matrix. Although the modification of sage

did not significantly affect the content of polyphenolic compounds and diterpenes, it is believed that it impacted the content of its volatile oils. This highly influences the mechanical behavior of the composites. Similar behavior is observed for sage extract composites. Nonetheless, statis-

Table 3. Multi-criteria analysis

Property	Weight	Material													
		Ref		US55		US10		MS5		MS10		ES5		ES10	
		C	V	C	V	C	V	C	V	C	V	C	V	C	V
Density	1	7	7	6	6	5	5	2	2	1	1	3	3	4	4
Hardness	2	7	14	2	4	1	2	6	12	5	10	3	6	4	8
Rebound resilience	3	5	15	2	6	1	3	4	12	3	9	6	18	7	21
Strength at break	5	7	35	2	10	1	5	6	30	5	25	4	20	3	15
Elongation at break	4	7	28	1	4	2	8	4	16	6	24	3	12	5	20
Σ			99		30		23		72		69		59		68

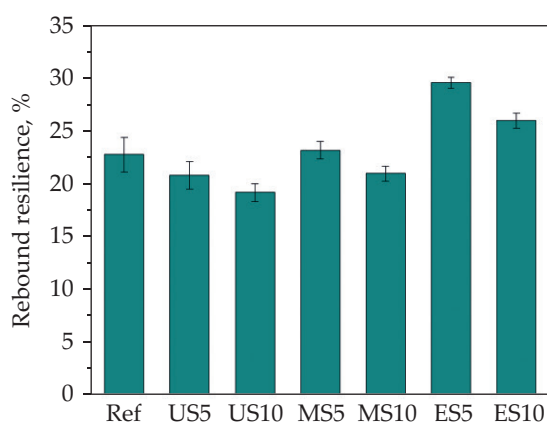


Fig. 8. The effect of the fillers on PDMS rebound resilience

tical significance of the filler type and content was found ($F(6,28) = 3.78, p < 0.05$).

Rebound resilience

The rebound resilience value of the tested composites varies depending on the filler type and fraction (Fig. 8). An inverse proportional dependence of resilience on the fraction is observed – the higher the filler content, the lower the value. The highest decrease is observed for raw sage composites, while the modification of the herb contributed to a smaller decrease in rebound resilience. This could be because the unmodified sage composites had large woody parts that were discarded after modification. Moreover, wetting with ethanol decreased the volatile oils in sage. Nevertheless, the herb-filled composites have lower rebound resilience values than sage extract-filled materials. This is attributable to the hygroscopic character of the herb, leading to moisture absorption, which causes the deterioration of the mechanical properties. The statistical analysis shows a strong dependency of the filler type and content on the rebound resilience values $F(6,28) = 62.08, p < 0.05$.

Tensile properties

The incorporation of the fillers affected the mechanical properties of PDMS. However, the tension characteristic of the matrix material remained unchanged, as shown

in Fig. 9. All composites exhibit an unequivocal correlation between the filler content and the degree of value decrease (Fig. 10). The most significant drop in tensile strength value is observed for US5 and US10 (52% and 58%, respectively). This is related to high crude fat content impacting the cross-linking of PDMS, which weakens the material [32]. Moreover, during tension, coarse grains tended to detach, thus creating a void that acted like a notch. On the other hand, MS5 and MS10 exhibit a smaller decrease, 14% and 26%, respectively. This proves the beneficial effect of the proposed herb in terms of the tensile strength properties. For sage extract composites, the decrease was up to 23% for ES5 and 27% for ES10. This leads to the conclusion that the polyphenolic compounds found in the extract impact the mechanical properties of PDMS. Although the obtained materials are characterized by lower tensile strength, the values of modified sage and sage extract composites fall within the range of values obtained by other researchers [33–35]. The statistical analysis proved the significance of the filler type and content on the tested property $F(6,28) = 21.61, p < 0.05$.

Much like tensile strength, elongation at break value (Fig. 11) drops after the incorporation of fillers. However, an inverse relation between the filler content and the degree of decrease is observed, i.e., the higher the content, the less the decrease. This could be related to the nature of the fillers, whereby the developed surface

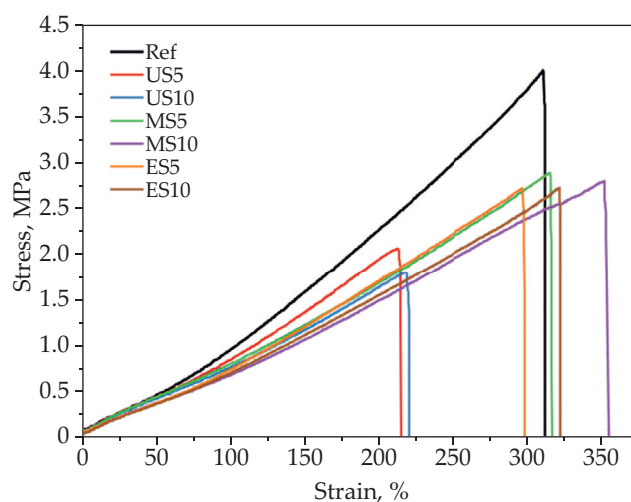


Fig. 9. Stress-strain curves of PDMS composites

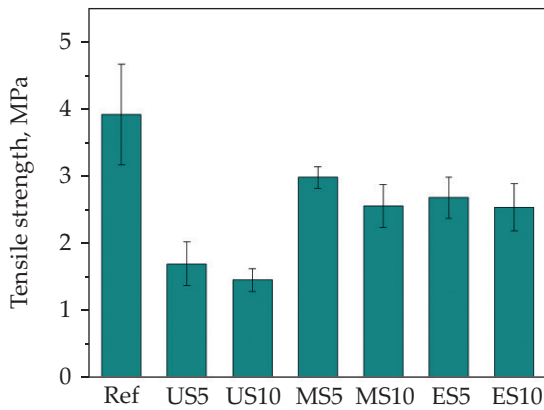


Fig. 10. The effect of the fillers on PDMS tensile strength

ensured a mechanical adhesion between the grains and the matrix. The drop in value is observed for all composites except for MS10, where an increase can be seen. The even distribution of grains for modified sage composites contributed to higher elongation at break values compared to the remaining fillers. Elongation at break – $F(6,28) = 8.32, p < 0.05$.

Multi-criteria analysis

Multiple-criteria analysis was carried out to assess the acquired materials (Table 3), where C – criterion and V – value. The assessment was based on the properties' results. Composites with the highest scores were subjected to antibacterial activity test in the following step. The weights were associated with the characteristics' impact on the materials' operational properties.

Based on the conducted multi-criteria analysis, composites filled with modified sage had higher characteristics among the tested composites. However, in relation

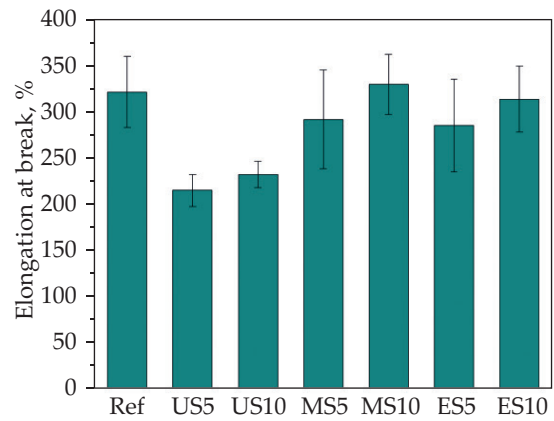


Fig. 11. The effect of the fillers on PDMS elongation at break

to this work's aim, the material with the highest content of sage extract was evaluated for antibacterial activity.

Antibacterial activity assessment

Modified sage composites exhibit antibacterial activity against *S. aureus* strain (Fig. 12a). The inhibition zone is bigger for MS10, indicating that the higher the filler content, the higher the antimicrobial activity of the material (Table 4). However, no inhibition zone is observed against *E. coli*, as seen in figure 12b). Gram-negative bacteria have an additional outer lipid layer, which protects them from outside factors, making it harder for bioactive substances to disrupt cell structures [36]. No antibacterial activity was observed for the composite incorporated with 10 wt.% of sage polyphenolic extract for both reference strains. Although sage extract contains rosmarinic acid, which is known to have strong antimicrobial properties, the composites did not exhibit antibacterial activity [37]. This allows to deduce that diterpenes (absent in the polyphenolic extract) exhibit sig-

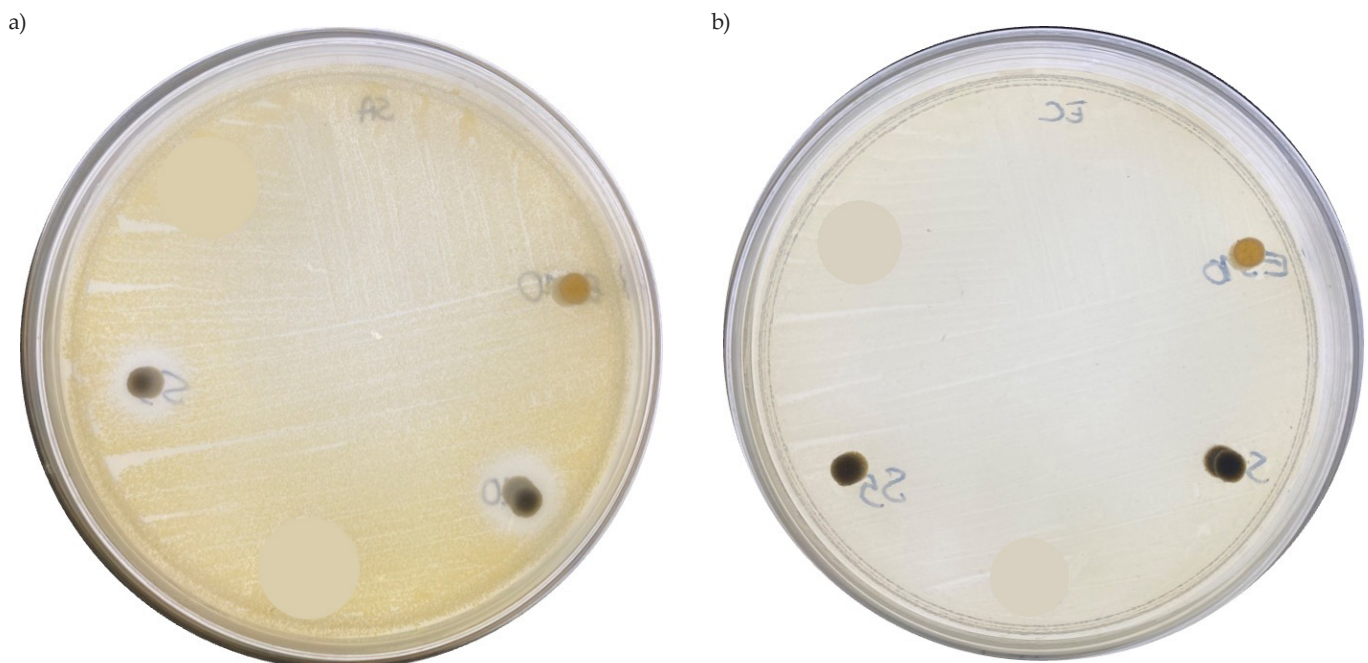


Fig. 12. Kirby-Bauer test results: a) *S. aureus*, b) *E. coli*

nificant antimicrobial properties in the case of the tested herb. However, it should be highlighted that the actual amount of polyphenolic extract in the obtained composites is around 10 times less than that of the herbal composites (mentioned in the preparation section).

T a b l e 4. Inhibition zone results

Material	Inhibition zone, mm	
	<i>S. aureus</i>	<i>E. coli</i>
MS5	10	–
MS10	13	–
ES10	–	–

CONCLUSIONS

Composites of polydimethylsiloxane with the addition of sage were obtained (raw herb, modified with ethanol, polyphenol extract). Modification of sage did not change its phytochemical composition but resulted in higher mechanical strength of PDMS necessary for wound dressing applications. The sage polyphenol extract decreased the mechanical properties of the composites, which may be the result of the presence of polyphenolic compounds. Moreover, the lack of crude fat in the extract reduced the antibacterial effect against *S. aureus*.

REFERENCES

- [1] Borda L.J., Macquhae F.E., Kirsner R.S.: *Current Dermatology Reports* **2016**, 5, 287. <https://doi.org/10.1007/s13671-016-0162-5>
- [2] Ranjan A., Shaik S., Nandanwar N. *et al.*: *mBio* **2017**, 8(4). <https://doi.org/10.1128/mbio.01070-17>
- [3] Dhivya S., Padma V.V., Santhini E.: *Biomedicine* **2015**, 5, 22. <https://doi.org/10.7603/s40681-015-0022-9>
- [4] Victor A, Ribeiro J., Araújo F.: *Journal of Mechanical Engineering and Biomechanics* **2019**, 4(1), 1. <https://doi.org/10.24243/JMEB/4.1.163>
- [5] Curtis J., Colas A.: „Medical Applications of Silicones“ in “Biomaterials Science: An Introduction to Materials“ (Eds. Ratner B., Hoffman A., Schoen F. *et al.*) Academic, Waltham 2013, p. 1106.
- [6] Shi G., Wang Y., Derakhshanfar S. *et al.*: *Materials Science and Engineering: C* **2019**, 100, 915. <https://doi.org/10.1016/j.msec.2019.03.058>
- [7] Li F., Han X., Cao D. *et al.*: *Frontiers of Material Science* **2023** 17, 230641. <https://doi.org/10.1007/s11706-023-0641-0>
- [8] Wang T., Lu Z., Wang X. *et al.*: *Applied Surface Science* **2021**, 550, 149286. <https://doi.org/10.1016/j.apsusc.2021.149286>
- [9] Bovis M., Noimark S., Woodhams J. *et al.*: *RSC Advances* **2015**, 5, 54830. <https://doi.org/10.1039/C5RA09045H>
- [10] Meran Z., Besinis A., De Peralta T. *et al.*: *Journal of Biomedical Research Part B: Applied Biomaterials* **2018**, 106(3), 1038. <https://doi.org/10.1002/jbm.b.33917>
- [11] Zong Y., Gui D., Li Si. *et al.*: *16th International Conference on Electronic Packaging Technology (ICEPT)* **2015**, 30. <https://doi.org/10.1109/icept.2015.7236538>
- [12] Fang L., Chen H.: *Polymer-Plastics Technology and Engineering* **2017**, 56(18), 1969. <https://doi.org/10.1080/03602559.2017.1298796>
- [13] Montemezzo M., Ferrari M.D., Kerstner E. *et al.*: *Journal of Biomaterials Applications* **2021**, 36(2), 252. <https://doi.org/10.1177/08853282211011921>
- [14] Jiao J., Sun L., Guo Z. *et al.*: *Scientific Reports* **2016**, 6, 38973. <https://doi.org/10.1038/srep38973>
- [15] Muangman P., Aramwit P., Palapinyo S. *et al.*: *African Journal of Pharmacy and Pharmacology* **2011**, 5(3), 442. <https://doi.org/10.5897/AJPP10.282>
- [16] Surakunprapha P., Winaikosol K., Chowchuen B. *et al.*: *Journal of Wound Care* **2020**, 29, 36. <https://doi.org/10.12968/jowc.2020.29.Sup4.S36>
- [17] Daniel Carrizo D., Giuseppe Gullo G., Osvaldo Bosetti O. *et al.*: *Food Additives and Contaminants: Part A* **2014**, 31(3), 364. <https://doi.org/10.1080/19440049.2013.869361>
- [18] Sarraj S., Szymiczek M., Jurczyk S.: *Polymers* **2023**, 15(1), 42. <https://doi.org/10.3390/polym15010042>
- [19] Zayed S., Alshimy A., Fahmy A.E.: *International Journal of Biomaterials* **2014**, Article ID 750398. <https://doi.org/10.1155/2014/750398>
- [20] Ahmed A., Ali M.: *Journal of Research in Medical and Dental Science* **2021**, 9(12), 59.
- [21] Moş I., Micle O., Zdrâncă M. *et al.*: *Farmacia* **2010**, 58(5), 637.
- [22] Tsige Y., Tadesse S., Eyesus T.G. *et al.*: *Journal of Pathogens* **2020**, Article ID 3168325. <https://doi.org/10.1155/2020/3168325>
- [23] Roy S., Santra S., Das A. *et al.*: *Annals of surgery* **2020**, 271(6), 1174. <https://doi.org/10.1097/SLA.0000000000003053>
- [24] Serrano C.A., Villena G.K., Rodriguez E.F. *et al.*: *Scientific Reports* **2023**, 13, 10714. <https://doi.org/10.1038/s41598-023-37830-6>
- [25] Chen H., Zhang Q., Wang X. *et al.*: *Phytochemical Analysis* **2010**, 22(3), 247. <https://doi.org/10.1002/pca.1272>
- [26] Sharma Y., Velamuri R., Fagan J. *et al.*: *Pharmacognosy Research* **2020**, 12(2), 149. https://doi.org/10.4103/pr.pr_92_19
- [27] Koutsoulas A., Carnecka M., Slanina J. *et al.*: *Molecules* **2019**, 24(16), 2921. <https://doi.org/10.3390/molecules24162921>
- [28] Liu C., Du L., Zhang S. *et al.*: *Frontiers in Pharmacology* **2023**, 14, 1108518. <https://doi.org/10.3389/fphar.2023.1108518>

- [29] Velamuri R., Sharma Y., Fagan J. *et al.*: *Planta Medica International Open* **2020**, 7, e133–e144.
<https://doi.org/10.1055/a-1272-2903>
- [30] Karolak I., Krzeminska M., Kiss A.K. *et al.*: *Metabolites* **2020**, 10(12), 497.
<https://doi.org/10.3390/metabo10120497>
- [31] Mehmood S., Riaz N., Nawaz S.A. *et al.*: *Archives of Pharmacal Research* **2006**, 29, 195.
<https://doi.org/10.1007/BF02969392>
- [32] Sadowska U., Kopec A., Kourimska L. *et al.*: *Journal of Food Processing and Preservation* **2017**, 41(6), e13286.
<https://doi.org/10.1111/jfpp.13286>
- [33] Lee E., Zhang H., Jackson J. *et al.*: *RSC Advanced* **2016**, 83, 79900.
<https://doi.org/10.1039/C6RA16232K>
- [34] Qian W., Hu X., He W. *et al.*: *Colloids and Surfaces B: Biointerfaces* **2018**, 166, 61.
<https://doi.org/10.1016/j.colsurfb.2018.03.008>
- [35] Wang H., Duan W., Ren Z.: *Advanced Healthcare Materials* **2023**, 12(8), 2202685.
<https://doi.org/10.1002/adhm.202202685>
- [36] Liu B., Furevi A., Perepelov A. *et al.*: *FEMS Microbiology Reviews* **2020**, 44(6), 655.
<https://doi.org/10.1093/femsre/fuz028>
- [37] Hitl M., Kladar N., Gavarić N. *et al.*: *Planta Medica* **2021**, 87(4), 273.
<https://doi.org/10.1055/a-1301-8648>

Received 28 XI 2023.


 Fundacja
TYGIEL

zaprasza do udziału w

VIII Ogólnopolskiej Konferencji Naukowej „NANOTECHNOLOGIA WOBEC OCZEKIWAŃ XXI w.” 9 maja 2024 r., online

Nanotechnologia, jako nauka zajmująca się tworzeniem struktur na poziomie atomów i cząsteczek, wpisuje się w trend miniaturyzacji, który niewątpliwie jest odpowiedzią na potrzeby dzisiejszego społeczeństwa. Możliwość wytwarzania nanocząsteczek oraz projektowania złożonych nanostruktur, tak aby wykazywały pożądane właściwości fizyczne, chemiczne, czy też biologiczne pokazuje, jak duży potencjał niesie ze sobą ta nauka.

Celem Konferencji, organizowanej przez Fundację na rzecz promocji nauki i rozwoju TYGIEL, jest przybliżenie wiedzy oraz najnowszych osiągnięć naukowych w zakresie nanotechnologii. Podczas spotkania poruszone zostaną kwestie zarówno tworzenia nanomateriałów, jak i wykorzystania osiągnięć nanotechnologii w obrębie technologii, przemysłu oraz medycyny. Udział w Konferencji przyczyni się nie tylko do wymiany doświadczeń, ale stanie się także inspiracją do dalszych badań.

Tematyka konferencji:

- metody wytwarzania i właściwości nanocząsteczek,
- tworzenie i funkcjonalizacja nanostruktur,
- charakteryzacja nanostruktur,
- właściwości i zastosowanie nanomateriałów,
- bezpieczeństwo wytwarzania, składowania i wykorzystania nanostruktur,
- aspekty etyczne, prawne i społeczne tworzenia oraz wykorzystania nanostruktur,
- komercjalizacja wyników i nowych technologii z zakresu nanotechnologii.

Ważne terminy:

Zgłoszenie udziału:

I etap – 13 lutego 2024 r., **II etap** – 14 marca 2024 r., **III etap** – 25 kwietnia 2024 r.

Przysłanie streszczenia wystąpienia – 9 maja 2024 r.

Przysłanie pełnego tekstu wystąpienia – 27 maja 2024 r.

Wydanie monografii – 20 września 2024 r.

Miejsce konferencji: platforma ClickMeeting – online

Kontakt: technologie@fundacja-tygiel.pl, tel.: 733 933 416

<https://konferencja-nanotechnologia.pl/>